ISSN 1674-1056
http://cpb.iphy.ac.cn
http://iopscience.iop.org/cpb
中国物理 B
Chinese Physics
中国物理
Chinese Physics B

High-gradient magnetic field-controlled migration of solutes and particles and their effects on solidification microstructure: A review

Tie Liu(刘铁), Qiang Wang(王强), Yi Yuan(苑轶), Kai Wang(王凯), Guojian Li(李国建)

Citation: Chin. Phys. B . 2018, 27(11): 118103. **doi:** 10.1088/1674-1056/27/118103
Journal homepage: http://cpb.iphy.ac.cn; http://iopscience.iop.org/cpb

What follows is a list of articles you may be interested in

A lattice Boltzmann-cellular automaton study on dendrite growth with melt convection in solidification of ternary alloys

Dong-Ke Sun(孙东科), Zhen-Hua Chai(柴振华), Qian Li(李谦), Guang Lin(林光)
Chin. Phys. B . 2018, 27(8): 088105. **doi:** 10.1088/1674-1056/27/8/088105

Effects of physical parameters on the cell-to-dendrite transition in directional solidification

Wei Lei, Lin Xin, Wang Meng, Huang Wei-Dong
Chin. Phys. B . 2015, 24(7): 078108. **doi:** 10.1088/1674-1056/24/7/078108

Tip-splitting instability in directional solidification based on bias field method

You Jia-Xue, Wang Zhi-Jun, Li Jun-Jie, Wang Jin-Cheng
Chin. Phys. B . 2015, 24(7): 078107. **doi:** 10.1088/1674-1056/24/7/078107

Dendrite to symmetry-broken dendrite transition in directional solidification of non-axially oriented crystals

Xing Hui, Wang Jian-Yuan, Chen Chang-Le, Jin Ke-Xin, Du Li-Fei
Chin. Phys. B . 2014, 23(3): 038104. **doi:** 10.1088/1674-1056/23/3/038104

A steady solution of the gasar eutectic growth in directional solidification

Li Xiang-Ming, Li Wen-Qiong, Jin Qing-Lin, Zhou Rong
Chin. Phys. B . 2013, 22(7): 078101. **doi:** 10.1088/1674-1056/22/7/078101

TOPICAL REVIEW — Fundamental research under high magnetic fields

High-gradient magnetic field-controlled migration of solutes and particles and their effects on solidification microstructure: A review*

Tie Liu(刘铁)[1], Qiang Wang(王强)[1,†], Yi Yuan(苑轶)[1,2], Kai Wang(王凯)[1], and Guojian Li(李国建)[1]

[1] *Key Laboratory of Electromagnetic Processing of Materials (Ministry of Education), Northeastern University, Shenyang* 110819, *China*
[2] *School of Metallurgy, Northeastern University, Shenyang* 110819, *China*

(Received 30 July 2018; published online 19 October 2018)

We present a review of the principal developments in the evolution and synergism of solute and particle migration in a liquid melt in high-gradient magnetic fields and we also describe their effects on the solidification microstructure of alloys. Diverse areas relevant to various aspects of theory and applications of high-gradient magnetic field-controlled migration of solutes and particles are surveyed. They include introduction, high-gradient magnetic field effects, migration behavior of solute and particles in high-gradient magnetic fields, microstructure evolution induced by high-gradient magnetic field-controlled migrations of solute and particles, and properties of materials modified by high-gradient magnetic field-tailored microstructure. Selected examples of binary and multiphase alloy systems are presented and examined, with the main focus on the correlation between the high-gradient magnetic field-modified migration and the related solidification microstructure evolution. Particular attention is given to the mechanisms responsible for the microstructure evolution induced by high-gradient magnetic fields.

Keywords: high gradient magnetic field, migration of solute and particle, solidification, microstructure

PACS: 81.30.Fb, 64.70.kd, 64.75.Op **DOI:** 10.1088/1674-1056/27/11/118103

1. Introduction

The control of microstructure formation during solidification is becoming increasingly important for a wide variety of technical and scientific applications because a strong relationship exists between the performance of a material and its microstructure.[1,2] Developments in science and technology rely heavily on the development of new materials systems with highly modified or newly designed microstructures that can meet the requirements of advancing technology. One of the most important processing routes for many materials, by which microstructure control and design can be accomplished, is solidification.[3] In recent years, high magnetic fields have been applied in materials processing, especially in solidification, as a non-contact method to more precisely control the material microstructure.[4–7] It has been found that the microstructure is strongly dependent on the migration behaviors of solutes and particles (or particle-like phases), so a comprehensive understanding of the evolution of the migration behaviors of solutes and particles during solidification processes in high magnetic fields is essential for the prediction and control of the final microstructures and properties of materials.[8] Several studies have investigated the effects of high magnetic fields on migrations of solutes and particles in alloy melts during solidification[9–11] and some research has specifically been directed to the effects of high-gradient magnetic fields. The results have indicated that the migrations of solutes and particles exhibit different behaviors in high-gradient magnetic fields compared with those under normal conditions.

Under high-gradient magnetic field conditions, modifications of solute and particle migrations occur due to magnetic forces, the Lorentz force, thermoelectromagnetic force (TEMF, a special kind of Lorentz force), magnetic torque, and magnetic dipole–dipole interactions. Of these, the magnetic force shows the most powerful ability to control the migrations of both solutes and particles. The magnetic force is induced by the interaction of the magnetization of materials and the imposed magnetic field gradient and is proportional to the volume of the considered materials and the product of the magnetic flux density and its gradient. For a solid/liquid system in a gradient magnetic field, the magnetic influence of the liquid can also produce a so-called magneto-Archimedes buoyant force on the solid materials, which can strongly enhance the magnetic field effect.[12] Thus, by increasing the magnetic flux density and carefully designing the materials systems, the magnetic force can be strongly enhanced and even give rise to obvious effects on materials with weak magnetic susceptibility and small size. This is very important for solidification pro-

*Project supported by the National Natural Science Foundation of China (Grant Nos. 51425401, 51690161, 51574073, and 51774086), Fundamental Research Funds for the Central Universities, China (Grant Nos. N170902002 and N170908001), and Liaoning Innovative Research Team in University, China (Grant No. LT2017011).

†Corresponding author. E-mail: wangq@epm.neu.edu.cn

© 2018 Chinese Physical Society and IOP Publishing Ltd

cesses because at elevated temperatures, especially above the melting point temperatures, the magnetic properties become very weak, even for ferromagnetic materials.

Because microstructure is directly related to migrations of the solute and solid phases, research has been extended to understanding the evolution of solidification microstructures under migrations that are modified by gradient magnetic fields. The results suggest that the attendant migration phenomena induced by high-gradient magnetic fields can have profound impacts on the distribution of alloying elements and their product phases in materials during the solidification process. By coupling the magnetic force with other magnetic field effects—i.e., Lorentz force, TEMF, magnetic torque, and magnetic dipole–dipole interaction—segregation on both the micro- and macro-scales is strongly suppressed and a series of layered and graded composite structures (sometimes having a crystallographic orientation or morphological alignment) have been fabricated *in situ*. The possibility then arises of a direct processing route using *in situ* control of solute and particle migrations during solidification of alloys and thus control of solidification microstructure by high-gradient magnetic fields.

This review describes the fundamentals regarding the evolution and synergism of solute and particle migration in a liquid melt in high-gradient magnetic fields. Selected examples of binary and multiphase alloy systems are presented and examined, with the main focus on the correlation between the high-gradient magnetic field-modified migration and the related solidification microstructure evolution. Particular attention is paid to the mechanisms responsible for the microstructure evolution induced by high-gradient magnetic fields.

2. Effects of a high-gradient magnetic field on materials

From the point of view of controlling the migrations of solute and particles during a solidification process, a high-gradient magnetic field mainly exhibits five effects; i.e., magnetic force, Lorentz force, TEMF, magnetic torque, and magnetic dipole–dipole interaction. A brief introduction to the origins of these effects is given.

2.1. Magnetic force

It is well-established that when a nonmagnetic substance is subjected to a magnetic field gradient, it will be acted upon by a magnetic force due to the interaction of the magnetization and the imposed magnetic field gradient. Depending on the magnetic property of the material, the direction of the induced magnetic force can be either along or opposite to the magnetic field gradient for paramagnetism or antimagnetism, respectively. In practical applications, a longitudinal gradient magnetic field is usually applied, which imposes a magnetic force on the material in the direction along or opposite to that of gravity, depending on its magnetic susceptibility. The z-axis component of the force can be expressed as

$$F = V(1/\mu_0)\chi B\mathrm{d}B/\mathrm{d}z, \tag{1}$$

where V is the volume of the substance, μ_0 is the vacuum permeability, χ is the magnetic susceptibility per unit volume, and B is the magnetic flux density along the z direction.

When this simple description is extrapolated to a binary system consisting of a liquid matrix M and dispersed particles P of different magnetic susceptibilities, the resultant force acting on P, with consideration of the buoyancy effect, can be given by[12]

$$\begin{aligned} F_{\mathrm{P}} &= V_{\mathrm{P}}(\chi_{\mathrm{P}} - \chi_{\mathrm{M}})\frac{1}{\mu_0}B\frac{\mathrm{d}B}{\mathrm{d}z} \\ &\quad - (\rho_{\mathrm{P}} - \rho_{\mathrm{M}})V_{\mathrm{P}}g, \end{aligned} \tag{2}$$

where ρ is the density and g is the gravitational acceleration in the z direction. Supposing that the absolute susceptibility of P is larger than that of M, then if the value of $B\mathrm{d}B/\mathrm{d}z$ is high enough, M tends to migrate in the matrix along the direction (a positive susceptibility) or opposite to the direction (a negative susceptibility) of the magnetic force.

2.2. Lorentz force

In a magnetic field, if there is an electric current caused by the movement of an electrically conducting or partially electrically conducting fluid in the field, a Lorentz force will be produced by the interaction of the electric current and the applied magnetic field. The Lorentz force is given by

$$\boldsymbol{F}_{\mathrm{L}} = \boldsymbol{J} \times \boldsymbol{B} = \sigma(\boldsymbol{u} \times \boldsymbol{B}) \times \boldsymbol{B}, \tag{3}$$

where σ is the conductivity of the fluid, $\boldsymbol{u}$ is the velocity of the fluid, and $\boldsymbol{J}$ is the effective electric current.

2.3. Thermoelectromagnetic force

If there is a thermoelectric current at a liquid/solid interface caused by the Seebeck effect, then a TEMF will be produced by the interaction of the current and the applied magnetic field. For instance, during the growth of a dendrite in a magnetic field, an electric current $\boldsymbol{i}_{\mathrm{TE}}$ can be induced by a temperature difference between the solid dendrite and the remaining liquid phase, on the basis of the Seebeck effect. The TEMF can be given by[13]

$$F_{\mathrm{TEM}} = i_{\mathrm{TE}} \times \boldsymbol{B} = \frac{\sigma_{\mathrm{S}}\sigma_{\mathrm{L}}^2}{(\sigma_{\mathrm{S}} - \sigma_{\mathrm{L}})^2} f_{\mathrm{S}}(\xi_{\mathrm{S}} - \xi_{\mathrm{L}})\boldsymbol{\nabla} T \times \boldsymbol{B}, \tag{4}$$

where σ_{L} is the conductivity of the liquid, σ_{S} is the conductivity of the solid, ξ_{L} is the thermoelectric potential of the liquid, ξ_{S} is the thermoelectric potential of the solid, and f_{S} is the volume fraction of the solid.

2.4. Magnetic torque

When non-magnetic materials, such as paramagnetic and diamagnetic materials, are magnetized by a magnetic field, the material will be affected by the magnetic torque because the magnetization vector is not parallel to the magnetic field vector. The magnetic torque in the direction of the z axis can be expressed as[14]

$$L = \frac{V(\chi_1 - \chi_2)B^2 \sin 2\theta}{2\mu_0}, \tag{5}$$

where χ_1 (along the x axis) and χ_2 (along the y axis) are the magnetic susceptibilities in the easy and difficult magnetization axes, respectively, and θ denotes the angle between the easy magnetization axis and the imposed magnetic field direction.

2.5. Magnetic dipole–dipole interaction

When magnetic particles are placed in a magnetic field, the particles become magnetic dipoles because they are magnetized. The dipole–dipole interaction acts as a mutual attraction between the particles in the plane parallel to the magnetic field, while the particles in the plane perpendicular to the magnetic field exhibit mutual repulsion. Assuming that the particles are spherical, the interaction energy between two neighboring magnetic dipoles, m_1 and m_2, can be expressed as[15]

$$U_{\mathrm{M}} = \frac{\mu_0}{4\pi} \frac{l^2 \boldsymbol{q}_{\mathrm{m1}} \cdot \boldsymbol{q}_{\mathrm{m2}} - 3(\boldsymbol{q}_{\mathrm{m1}} \cdot \boldsymbol{l})(\boldsymbol{q}_{\mathrm{m2}} \cdot \boldsymbol{l})}{l^5}, \tag{6}$$

where $\boldsymbol{q}_{\mathrm{m1}}$ and $\boldsymbol{q}_{\mathrm{m2}}$ are the magnetic dipole moments of m_1 and m_2 magnetic dipoles, respectively, and $\boldsymbol{l}$ denotes the distance between the centers of particles m_1 and m_2.

When the particles are paramagnetic, the induced magnetic dipole moment can be expressed by the following formula:

$$\boldsymbol{q}_{\mathrm{m}} = \frac{\pi r_{\mathrm{p}}^3}{6} \mu_0 \chi_{\mathrm{e}} H_{\mathrm{ex}}, \tag{7}$$

where r_{p} is the radius of the particle, χ_{e} is the effective magnetic susceptibility of the particles, and H_{ex} is the magnetic field intensity of the imposed magnetic field.

3. Effects of high-gradient magnetic fields on migrations of solute and particles

It has been shown that magnetic susceptibility is dependent on the density of materials,[16] thus non-uniform distribution of solute during solidification of alloys, caused by a diffusion or temperature gradient, may induce a density gradient. According to Eq. (1), the magnetic force is also proportional to the magnetic susceptibility; thus, if there is a magnetic susceptibility gradient in an alloy melt, induced by the density gradient of solutes during the solidification process, the induced non-uniform magnetic force should cause fluid motion and alter the solute migration. This has been confirmed by research performed by Wang *et al.*[17] These researchers developed an optical system based on the Schlieren principle which can be used to observe fluid motion *in situ* in a transparent solution in magnetic fields up to 13 T. Choosing a crystal of diamagnetic aluminum potassium sulfate dodecahydrate as the model material, they observed a downward flow of high concentration solution during the dissolution process. They found that the direction of the diamagnetic fluid flow changed in high-gradient magnetic fields. Without a magnetic field, the dissolved solution flow moved straight down toward the bottom of the sample holder, whereas, with the magnetic field, this flow was slightly bent. This phenomenon was qualitatively understood by considering the magnetic force acting on the high concentration solution and the surrounding solution.

This research has mainly focused on controlling the fluid flow by high-gradient magnetic fields, which can indirectly alter the solute distribution. Other attempts have been made to directly control the migration behavior of alloying elements and their product phases in the melt during solidification by high-gradient magnetic fields. In practice, materials are generally binary or multiple systems consisting of different solutes or a mixture of a liquid matrix and dispersed particles, so the mechanism of such control is that the magneto-Archimedes buoyant force, originating from the magnetic susceptibility difference between the solutes or phases, can drive either the solute or particles to move in the alloy melt.

For systems consisting of a liquid matrix and solid particle-like phases, the phases may be formed *in situ* during cooling of the melt,[18] added in a preceding step,[19] or transformed during annealing in the semi-solid state.[20] When particles move at a velocity through a molten metal, which can be regarded as a viscous liquid, they will experience a hydrodynamic resistance of drag force from the melt. As shown in Fig. 1, with a high-gradient magnetic field, if the magneto-Archimedes buoyant force is larger than the drag force, then the particles can be driven to move in the direction of the force. Furthermore, the suppression effect of the Lorentz force on convection in a melt can eliminate additional migration of particles due to convection to maintain the effect of the magneto-Archimedes buoyant force. Because the magnetic force is proportional to the volume of the considered materials, control of the particle-like phase migration is easier because these phases cover a wide range of sizes due to their growth during the solidification process. This mechanism has been demonstrated by some experimental studies;[21–23] of these, migration of primary Si plate in an Al melt,[21] $TiAl_3$ particles in an Al/Si melt,[19] and primary MnSb particles in a Mn/Sb melt[20] were effectively controlled by high-gradient magnetic fields.

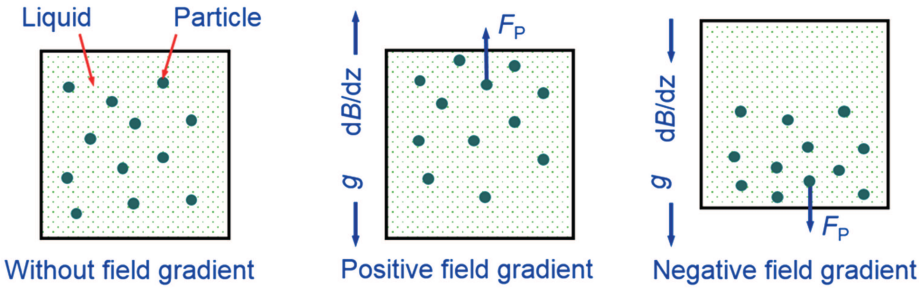


Fig. 1. (color online) Schematic illustration of particle migration with positive magnetic susceptibility driven by the magneto-Archimedes buoyant force F_P.[20]

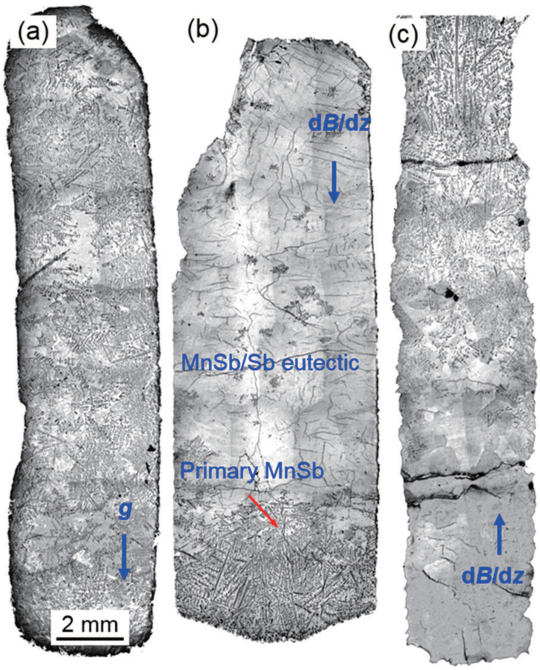


Fig. 2. (color online) Typical microstructures of Mn–89.7 mass% Sb alloys quenched at 590 °C after holding in various gradient magnetic fields ($B = 8.8$ T) of (a) $B\mathrm{d}B/\mathrm{d}z = 0$ T^2/m, (b) $B\mathrm{d}B/\mathrm{d}z = -565$ T^2/m, and (c) $B\mathrm{d}B/\mathrm{d}z = 400$ T^2/m (g is the gravitational acceleration).[26]

It is generally difficult to directly control solute migration in alloy melts by magnetic forces because such forces act on the particles at an atomic scale and, when resulting from a field of about 10 T, are so small that they cannot overcome the drag force from the melt. It has been widely accepted that, in liquid alloys, random fluctuations in concentration create minor short-range ordering domains, producing a large number of solute-enriched zones, even at temperatures far above the melting temperatures.[24,25] If the $|B\mathrm{d}B/\mathrm{d}z|$ value of a gradient magnetic field is large enough, then there is a high possibility that the magneto-Archimedes buoyant force induced by such a field can drive the solute-enriched zones to migrate along or opposite to the field direction and create a redistribution of solute in the alloy melt. This mechanism has been confirmed by experimental studies. Liu *et al.*[26] chose a Mn–Sb alloy system as the model material, the alloying elements of which—i.e., Mn and Sb—have a large difference in magnetic susceptibility in the liquid state (882.62×10^{-6} for Mn and -1.0048×10^{-6} for Sb[27,28]). They held the alloy melts in different high-gradient magnetic fields for various time and then quenched them to room temperature. On examining the distribution of the product phases—i.e., MnSb and Sb—in the quenched microstructure by quantitative metallography using an image analysis system, the migration behaviors of Mn in the melt in the high-gradient magnetic fields were characterized. The gradient magnetic field-dependent distribution of the MnSb phase observed from the quenched alloys indicated that the magneto-Archimedes buoyant force from a magnetic field of about 10 T was large enough to control the solute migration (Figs. 2 and 3). Further experiments have suggested that such control is dependent on the direction of the magnetic field gradient, the value of $|B\mathrm{d}B/\mathrm{d}z|$, holding temperature, and holding time.

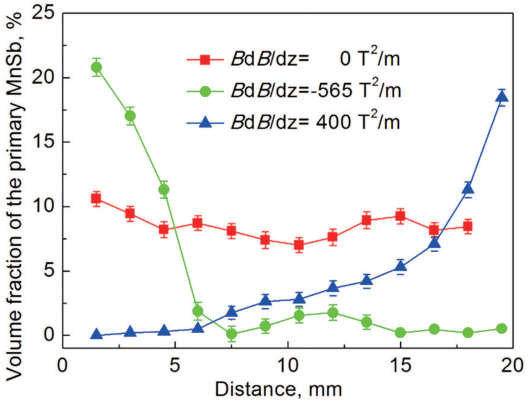


Fig. 3. (color online) Distributions of primary MnSb volume fraction along depth from the bottom of alloys quenched at 590 °C after holding in various gradient magnetic fields ($B = 8.8$ T).[26]

4. Microstructure evolution induced by high-gradient magnetic field-controlled migrations of solute and particles

The distribution of alloying elements and precipitated phases prior to or during solidification is of utmost importance when designing or controlling solidification microstructure of alloys.[29] Research on understanding the evolution of the migration of solutes and particles in high-gradient magnetic fields has tended to focus on exploring the design or control of alloys with such gradient magnetic field-modified mi-

grations. It is well-known that solute segregation, on either a macro- or micro-scale, in a solidified structure results in poor properties and performance of alloys.[30–33] For example, core segregation may not only induce differences in both physical and chemical properties on the scale of grains, but also have a marked impact on the mechanical properties of casting on a large scale; gravity segregation has a detrimental impact on subsequent processing behavior and properties of cast materials. Therefore, methods for control of segregation on both micro- and macro-scales in materials have been pursued.[34,35]

By coupling gradient magnetic fields with solidification conditions, migrations of solutes or phases in alloys during solidification have been modified and their distributions are thereby controlled to suppress solute segregation in the final structure. In many cases, especially in engineered materials, segregation may not even be desirable; however, it can provide good guidance for fabricating functional composite materials.[36] By manipulating the distribution of elements in alloys during solidification, a series of composite structures have been fabricated *in situ*, which have special characteristics and exhibit unique mechanical and physical properties. An excellent example is functionally graded materials (FGMs), the chemical composition and microstructure of which vary continuously and smoothly with depth from a free surface.[37] Because the magnetic force depends on the magnetic susceptibility and volume of the material on which the force acts, and most materials show weak magnetic susceptibility in the liquid state, the magnetic force has first been applied to phases having a relative larger volume, such as added phases, the primary phase of an eutectic system, or the product phases of the solute elements. Because the magnetic force is related to the magnetic flux density, application has also been extended to solute elements by adopting enhanced magnetic fields.

4.1. Control of sedimentation of phases and segregation of solutes

Migration of the solid phases in an alloy melt is strongly affected by natural convection.[38] It has long been recognized that the Lorentz force can significantly suppress thermal convection in a melt,[39–41] the sedimentation of phases in some alloys during solidification can therefore be obviously inhibited and more homogeneous microstructures can be obtained.[42–45] The associated efficiency is mainly dependent on the physical properties of density and electrical conductivity of the alloying elements.[46] Application of a gradient magnetic field provides another way to control migration of solid phases during solidification. This method is based on the magneto-Archimedes buoyant force, which is dependent on the magnetic susceptibility difference between the solid phases and liquid matrix.

In earlier examples, Al–Si alloys were chosen as model materials to demonstrate the controlling effects of a high-gradient magnetic field on the migration behavior of solid phases in an alloy melt. Wang *et al.*[21] applied such fields during solidification of a hypereutectic Al–Si alloy and successfully controlled segregation of the primary Si particles. A similar phenomenon was observed by Jin *et al.*[22] Following these studies, Lou *et al.*[19] compared the controlling efficiency of a high uniform magnetic field with that of a high-gradient magnetic field. They found that by coupling the magnetic and Lorentz forces, the gradient magnetic field gave better suppression of segregation of $TiAl_3$ particles in Al–7 mass% Si–0.5 mass% Ti alloys.

Gravitational segregation of the alloying elements in some alloys was similarly reduced by using high-gradient magnetic fields. For example, Cu and Mg are often segregated at the lower part of an Al–Cu alloy and the upper part of an Al–Mg alloy, respectively. The application of negative high-gradient magnetic fields was found to suppress such segregations more or less (Fig. 4). Such suppression was, however, strongly dependent on the direction of the field gradient: if a positive gradient was applied, the gravitational segregation in both alloys increased. These effects were dependent on the physical properties of the elements, such as magnetic susceptibility, density, and electrical conductivity.[47]

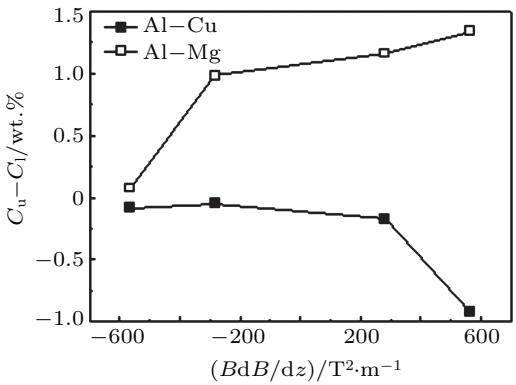


Fig. 4. (color online) Changes of $C_u - C_l$ of solutes in Al–5 mass% Cu and Al–10 mass% Mg alloys with $B\mathrm{d}B/\mathrm{d}z$. $C_u - C_l$ indicates the segregation extent, where C_u and C_l are the average elemental concentrations at the dendrite cores in the upper and lower parts of the specimens, respectively.[47]

4.2. Formation of particle- or phase-gathered microstructures with volume fraction gradients

By controlling the migration behavior of particle-like phases in alloys during solidification, particle- or phase-gathered microstructures with volume fraction gradients have been fabricated in several alloy systems. These may be formed *in situ* during cooling of the melt,[18] added in a preceding step,[19] or transformed during annealing treatment.[20] For example, during isothermal annealing in a high-gradient magnetic field, a hypoeutectic Mn–Sb alloy was first transformed to a semi-solid state to produce a mixture of a liquid matrix

and paramagnetic MnSb particles, migration of the MnSb particles in the liquid matrix in the field gradient direction was then triggered, and, finally, their distribution was successfully controlled to yield a particle concentration gradient (Fig. 5). The volume fraction distribution of MnSb particles throughout the alloy from the lower surface, as shown in Fig. 6, suggested that the concentration gradient varied from 0 to about 20% MnSb along the magnetic field gradient direction. Such control was dependent on the direction of the gradient, the value of $|B\mathrm{d}B/\mathrm{d}z|$, and annealing time.

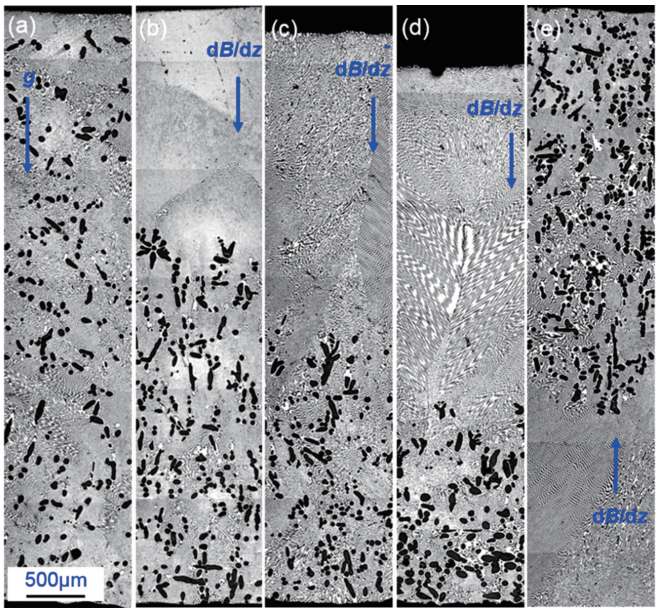


Fig. 5. (color online) Micrographs of MnSb/Sb–MnSb gradients in Mn–89.7 mass% Sb alloys annealed in different gradient magnetic fields and for various holding time. (a) 0 T and 30 min; (b) $B\mathrm{d}B/\mathrm{d}z = -114$ T^2/m and 30 min; (c) $B\mathrm{d}B/\mathrm{d}z = -282$ T^2/m and 30 min; (d) $B\mathrm{d}B/\mathrm{d}z = -282$ T^2/m and 90 min; (e) $B\mathrm{d}B/\mathrm{d}z = 282$ T^2/m and 30 min.

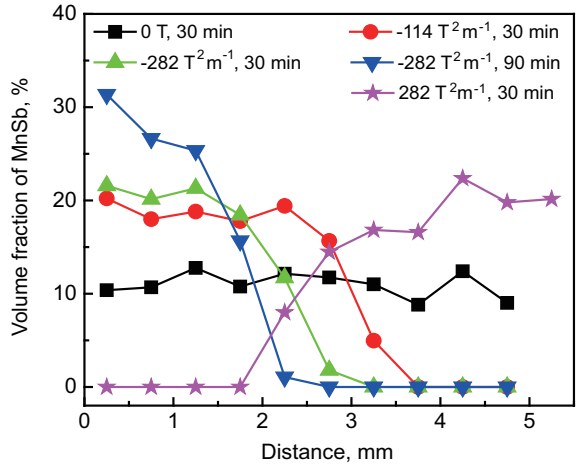


Fig. 6. (color online) Volume fraction distributions of MnSb particles along depth from the lower surface in Mn–89.7 mass% Sb alloys solidified at various magnetic field gradients for different annealing time.[20]

This approach has been extended to multiphase alloy systems, such as Al–12Si–11.8 Mg–6.5Ti, which has more than five different phases under equilibrium solidification conditions.[48] Liu *et al.* solidified this alloy in high-gradient magnetic fields at a relatively low cooling rate. They found that, with decreasing temperature, the primary Ti_5Si_4 particles, the primary $(Al,Si)_3Ti$ particles, the primary Mg_2Si, and the Al/Si eutectic precipitated in different temperature ranges and were driven by magnetic forces of different magnitudes and directions to move in the remaining melt for various times. Layered and graded distributions of these phases were formed in the final microstructure. Li *et al.*[49] carried out a similar investigation of a solidified Bi–Mn alloy in a radial gradient magnetic field, which produced a radially distributed magnetic force. During the solidification process, the precipitated primary MnBi phases were driven by the magnetic force and separated from the liquid Bi matrix to form a ring-like structure in the plane perpendicular to the magnetic field direction.

Quite recently, a symmetrically distributed gradient magnetic field was introduced to the forming of particle-gathered microstructures.[50] Such a field can produce symmetrically distributed magnetic forces. Choosing a hypoeutectic Mn–Sb alloy, a MnSb/Sb(eutectic)–MnSb(primary)–MnSb/Sb(eutectic) composite structure, with a symmetrically graded distribution in both morphology and composition, was directly fabricated *in situ*. Such composite structures were obtained during both solidification and isothermal annealing processes. Figure 7 shows the depth profile of the MnSb phase volume fraction measured from the top of the alloys solidified with and without a gradient magnetic field. Figure 8 shows a schematic diagram of the hypoeutectic Mn–Sb alloy isothermal annealing process and the curve of the stress state of the MnSb particles in the liquid melt in the symmetrically distributed high gradient magnetic field.

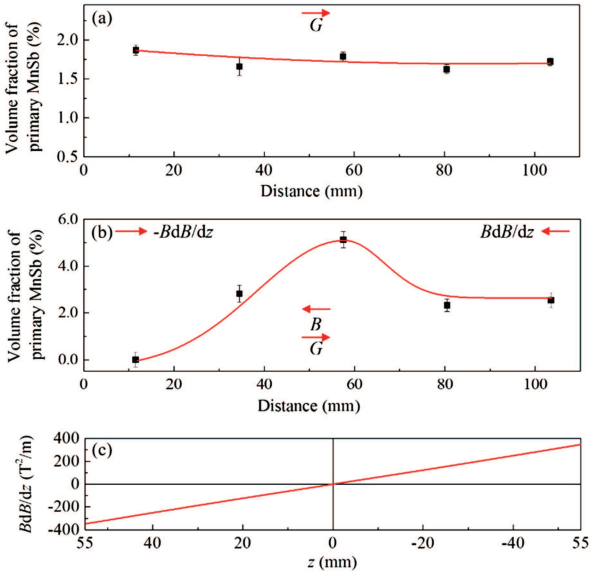


Fig. 7. (color online) Volume-fraction distribution of primary MnSb particles in Mn–89.7 mass% Sb specimens isothermally annealed (a) without and (b) with a symmetrically graded magnetic field of 12 T; (c) $B\mathrm{d}B/\mathrm{d}z$ distribution curve.[50]

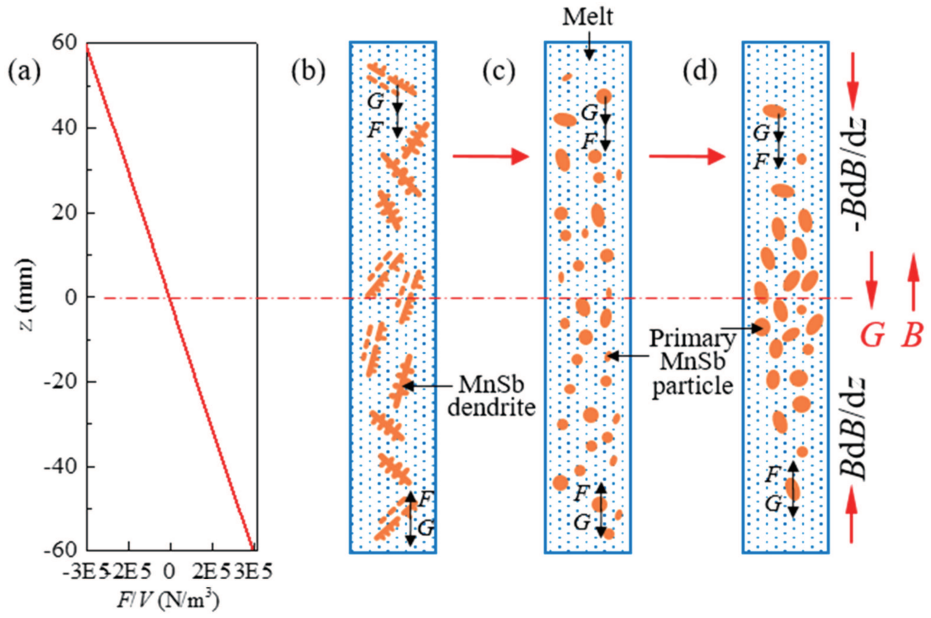


Fig. 8. (color online) (a) Stress state of Mn-enriched zones in liquid melt and (b)–(d) schematic diagram of Mn–89.7 mass% Sb alloy isothermal annealing process in symmetrically distributed high-gradient magnetic field (G is the gravity).[50]

4.3. Formation of layered microstructure with compositional gradients

Similar to that of the particle-like phases, if the solute migration both prior to or during a solidification process can be well-controlled, then the final microstructure of the alloys will be altered. This has support from some experimental results. As illustrated in Fig. 9, when a Mn–Sb melt with a eutectic composition is subjected to a gradient magnetic field, the magnetic force will drive the Mn-enriched zones to move along the gradient direction to form a Mn concentration gradient throughout the specimen, producing an extended alloy composition range in the binary Mn–Sb phase diagram, as indicated by the grid in Figs. 9(b) and 9(c). The solidification microstructure of the alloys will thus exhibit a continuous change in morphology due to the graded distribution of the solute concentration.[51] According to this mechanism, layered microstructural gradients have been produced from eutectic[51] and hypoeutectic[18] microstructures by controlling the solute distribution in high-gradient magnetic fields (Fig. 10). Three layers were produced by solidification of Mn–Sb alloys in high-gradient magnetic fields. Both the primary MnSb and Sb phases exhibited a continuous change in volume fraction in a metallic MnSb/Sb matrix and their locations depended on the direction of the field gradients (Fig. 11). The evolution of the microstructure was strongly dependent on the alloy composition, specimen dimension, cooling rate, and the $|B\mathrm{d}B/\mathrm{d}z|$ value.

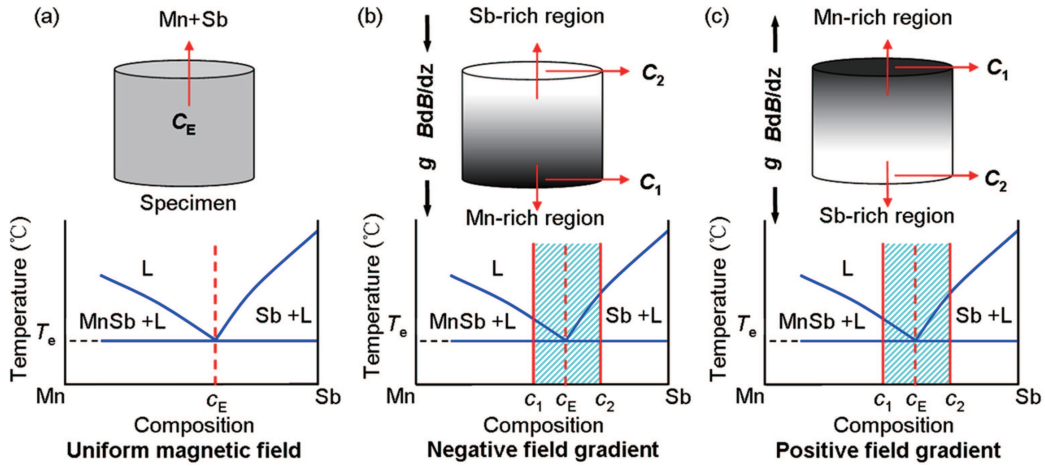


Fig. 9. (color online) Schematic diagrams of distributions of alloying elements in eutectic Mn–Sb melts prior to solidification in various gradient magnetic fields: (a) without magnetic field; (b) with a negative gradient field; (c) with a positive gradient field.[51]

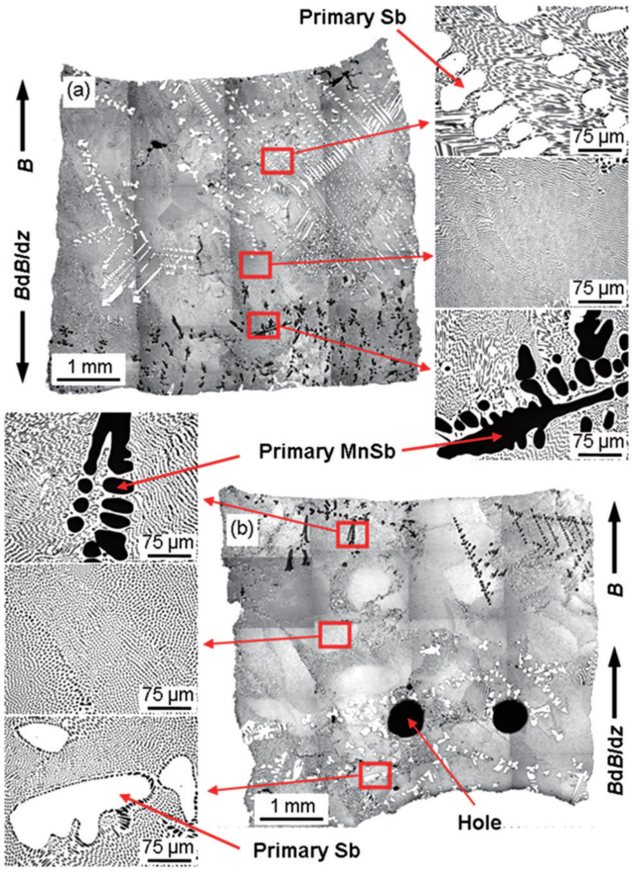


Fig. 10. (color online) Microstructures of eutectic Mn–Sb alloys solidified in gradient magnetic fields of (a) $B\mathrm{d}B/\mathrm{d}z = -282$ T^2/m and (b) $B\mathrm{d}B/\mathrm{d}z = 250$ T^2/m ($B = 11.5$ T). The alloy exhibited uniform eutectic microstructure in a high uniform magnetic field.[51]

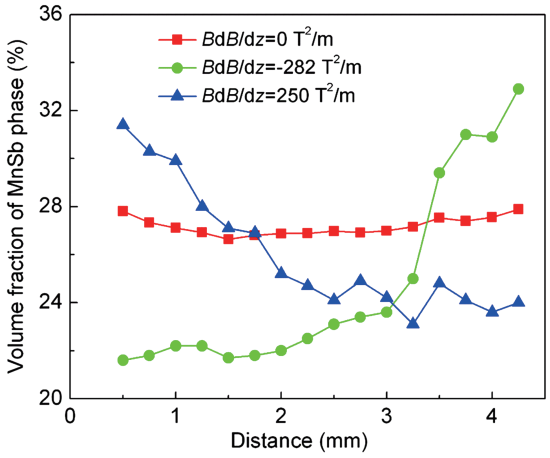


Fig. 11. (color online) Distributions of MnSb phase volume fraction along depth from the top surface of eutectic Mn–Sb alloys solidified in various gradient magnetic fields ($B = 11.5$ T).[51]

As an alternative to separately controlling the migration of solutes or particle-like phases, Liu *et al.*[52] chose a multiphase alloy system—i.e., Bi–11.8 mass% Mn—as the experimental material and explored the possibility of simultaneously controlling the migration of solutes and particles during the solidification process. This alloy has four phases (primary Mn, primary MnBi, eutectic Bi, and eutectic MnBi) that successively precipitate during the solidification process. They solidified the alloy in various high-gradient magnetic fields at a low cooling rate. By controlling the migrations of both the Mn solute and primary MnBi phase during solidification, a Bi/BiMn(eutectic)–BiMn(primary)–Mn(primary) layered microstructure was produced. The location of each layer changed with the direction of the magnetic field gradient (Fig. 12). The critical values of $-B\mathrm{d}B/\mathrm{d}z$ for levitation of the

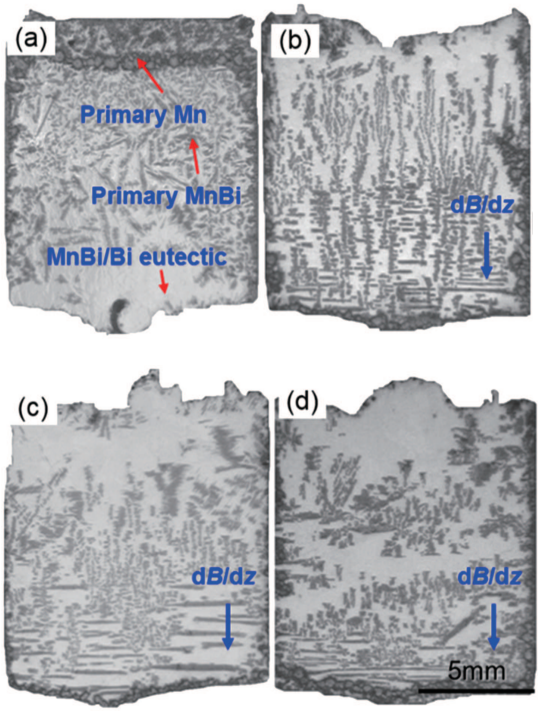


Fig. 12. (color online) Microstructures of Bi–11.8 mass% Mn alloys solidified in various high-gradient magnetic fields ($B = 8.6$ T): (a) $B = 0$ T; (b) $B\mathrm{d}B/\mathrm{d}z = -50$ T^2/m; (c) $B\mathrm{d}B/\mathrm{d}z = -100$ T^2/m; (d) $B\mathrm{d}B/\mathrm{d}z = -300$ T^2/m.[52]

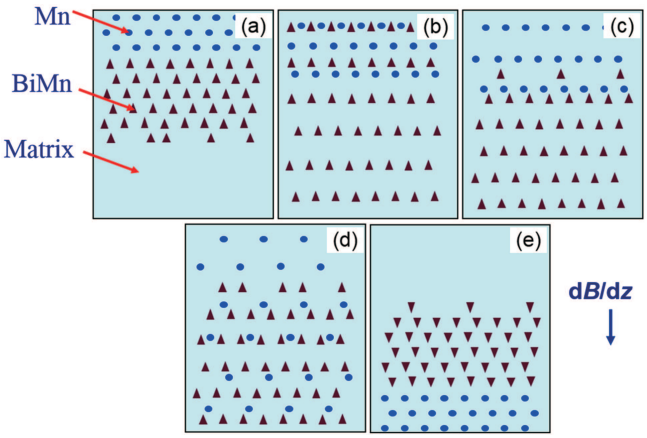


Fig. 13. (color online) Schematic diagrams of distributions of primary Mn and BiMn in various high-gradient magnetic fields: (a) without magnetic field, both primary Mn and BiMn segregated in the upper part; (b) $-B\mathrm{d}B/\mathrm{d}z \approx 6$ T^2/m, primary Mn was homogeneously distributed; (c) $6 < -B\mathrm{d}B/\mathrm{d}z < 14$ T^2/m, primary Mn segregated in the lower part; (d) $-B(\mathrm{d}B/\mathrm{d}z) \approx 14$ T^2/m, primary BiMn was homogeneously distributed; (e) $-B\mathrm{d}B/\mathrm{d}z \gg 14$ T^2/m, both primary Mn and BiMn strongly segregated in the lower part.[52]

Mn solute and BiMn phase were calculated using the model described in Ref. [21]. The distributions of the primary Mn and BiMn in the alloys in various gradient magnetic fields were predicted according to these calculated values (Fig. 13). The prediction confirmed that the migrations of solutes and particles can be simultaneously controlled.

4.4. Formation of graded microstructure with crystal orientation

Previous studies[53–55] have indicated that, when subjected to a magnetic field, a crystal with an anisotropic magnetic susceptibility, driven by the magnetic torque originating from the magnetic anisotropy, will rotate to an angle to give a certain crystal orientation. By incorporating the magnetic force with magnetic torque, the change of solute and particle migrations induced by high-gradient magnetic fields has also been suggested as a means to modify the growth of crystals with magnetically anisotropic features. Gao *et al.*[56] performed a series of solidification experiments on Tb–Dy–Fe alloys in various high-gradient magnetic fields to characterize their microstructure evolution. For the alloys solidified with and without a high uniform magnetic field, their saturation magnetization barely changed through their depth; however, for the alloys solidified in high-gradient magnetic fields, their saturation magnetization gradually increased from the top surface through the depth. Furthermore, the saturation magnetization increased in each section of the alloy more or less with increasing $B\mathrm{d}B/\mathrm{d}z$. In this alloy, (Tb, Dy)Fe_2 is the magnetic phase and the saturation magnetization of the alloy is strongly dependent on its proportion,[57–59] so the change in saturation magnetization thus indicated a gradient distribution of this phase throughout the alloy. The orientation degree of the (Tb, Dy)Fe_2 phase along the $\langle 111 \rangle$ direction, $F_{\langle 111 \rangle}$, was calculated from x-ray diffraction patterns measured from the transverse section of the solidified alloys using the model described in Ref. [60]. The calculation results showed that the applied high-gradient magnetic fields caused a graded increase of the orientation degree from the top surface through the depth. Furthermore, with increasing $B\mathrm{d}B/\mathrm{d}z$, the orientation degree increased for each part of the alloys. The $\langle 111 \rangle$ orientation of the (Tb, Dy)Fe_2 phase was induced by the magnetic field on the basis of this rotation. The gradient distributions of the orientation degree and phase amount throughout the alloy were due to migration of the precipitated (Tb, Dy)Fe_2 phase, driven by the gradient magnetic force during solidification under the high-magnetic field gradient. Further investigation indicated that the gradient magnetic field effect is strongly dependent on the cooling rate.[61]

Previous studies[62,63] have also suggested that, when exposed to a uniaxial magnetic field, suspended particles in a liquid matrix tend to orient along the applied field because of the increase of the magnetic dipole moment to which they are subjected. The particles will migrate under the influence of the magnetic dipole–dipole interactions between neighboring particles, which are either attractive or repulsive depending on the directions of the dipoles.[64,65] Wang *et al.*[66] characterized the evolution of the solidification microstructure of a Mn–Bi alloy in high-gradient magnetic fields. The MnBi grains aggregated strongly at one side of the specimen with a varying distribution throughout, yielding a highly aligned and graded microstructure. The formation of such a special microstructure was realized by incorporating the magnetic force with the magnetic dipole–dipole interactions. Because the alloy underwent a paramagnetic to ferromagnetic transformation during the solidification process,[67] the magnetic dipole–dipole interactions and the magnetic force caused a separation of the primary MnBi phase from the alloy melt and induced collision of particles, which thus resulted in the formation of the highly aligned and graded microstructure.

4.5. Degeneration of directionally solidified microstructure

During the growth of alloys or mixed or doped crystals, especially alloys that grow in a directional manner, a magnetic field can produce a TEMF, which can induce thermoelectric magnetic convection (TEMC) and cause migration of solutes.[68–71] Liquid motion due to TEMC can induce a Lorentz force that will, in turn, inhibit such motion to decrease the TEMC effect. Thus, there will be competition between the Lorentz force and TEMF in affecting convection, although this depends on the magnetic flux density.[72,73] If we apply a high-gradient magnetic field to the directional solidification of alloys, the field will affect the solidification in three ways, i.e., via the Lorentz force, TEMF, and magnetic force. These forces can produce a coupling effect on solute and particle migration and may generate a more complicated solidification microstructure. This has been demonstrated in some recent experimental studies.

Wu *et al.*[74] investigated the effects of a high-gradient magnetic field on the directional solidification of a hypereutectic Al–8 mass% Fe alloy. With the application of a gradient magnetic field, the primary Al_3Fe phase (that initially showed a directionally solidified morphology without application of a magnetic field) was twisted and fractured, some phases aggregated and distributed randomly in the samples to form a layered microstructure, and a eutectic area appeared at the top of the samples. The gradient magnetic field effect was dependent on the magnetic flux density (Fig. 14). The mechanism of this microstructural change was attributed to the magnetic force, which moved the Fe-enriched zones in the liquid matrix downward to the bottom of the samples during and even before

directional solidification. This migration is due to the TEMF, which caused a cross-flow in the front of the solid/liquid interface, and due to the Lorentz force, which suppressed convection to maintain the movement of the Fe-enriched zones induced by the magnetic force and to counteract the TEMF effect (Fig. 15). The coupling effect of these three forces thus caused deformation and fracture of the primary Al_3Fe phase, morphological instability in the interface between the eutectic area and the primary Al_3Fe phase, and random distribution of the aggregated primary Al_3Fe phase.

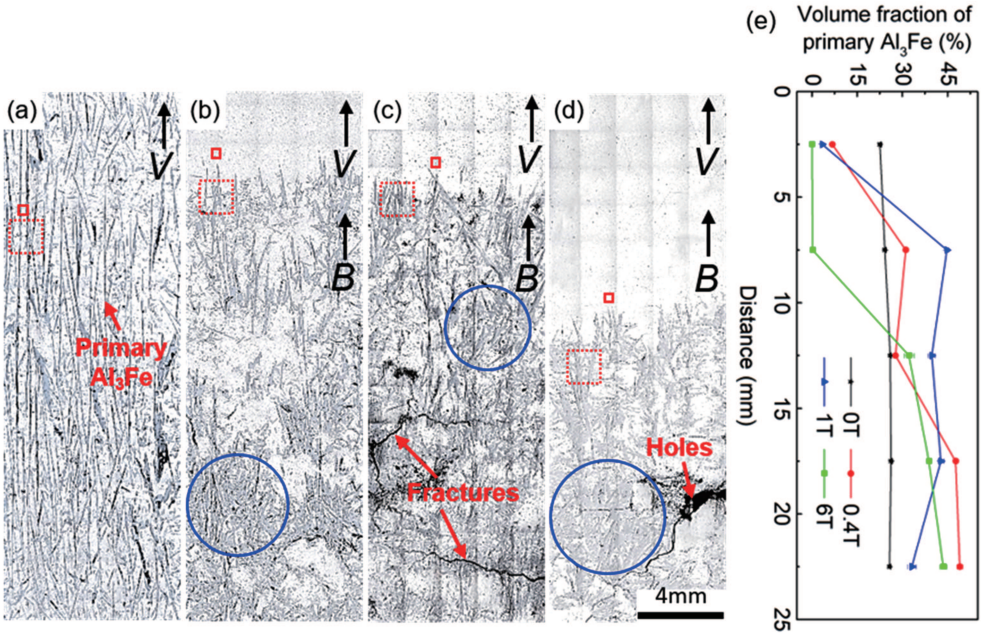


Fig. 14. (color online) Microstructure and volume fraction distribution in longitudinal section of directionally solidified Al–8 mass% Fe alloys grown in various magnetic fields: (a) 0 T; (b) 0.4 T; (c) 1 T; (d) 6 T. (e) Volume fraction distribution of the primary Al_3Fe phase. V is the growth rate. Reproduced from Ref. [74], with the permission of AIP Publishing.

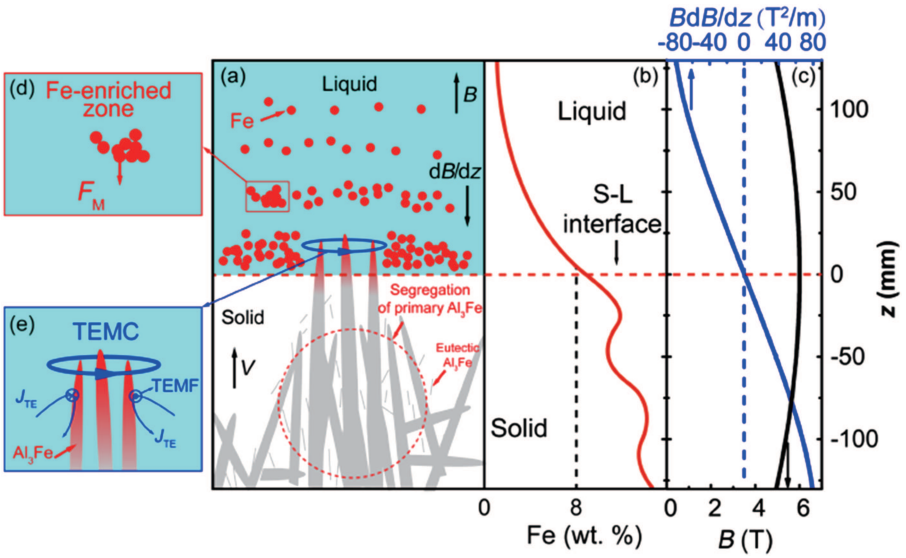


Fig. 15. (color online) Schematics of alloys during directional solidification under an applied magnetic field: (a) distribution of Fe atoms and microstructure of Al_3Fe phase as a liquid and solid under gradient magnetic field; (b) schematic of constitutional distribution; (c) distribution of magnetic flux density and its gradient along the axial direction; (d) schematic showing effect of magnetic force; (e) schematic showing the effect of TEMC. Reproduced from Ref. [74], with the permission of AIP Publishing.

5. Properties of materials modified by high-gradient magnetic field-tailored microstructure

The properties of materials have long been linked to their microstructure. To meet application demands for material properties, research has focused on the design and modification of microstructures. High-gradient magnetic fields have been shown to enable control of solute and particle migrations during solidification processes by combining several magnetic field effects, thereby creating some novel composite struc-

tures. These structures exhibit obvious effects on the properties of the resulting materials, especially the magnetic properties.

The intermetallic compound MnBi is ferromagnetic at room temperature and is proposed as a permanent magnet material.[75–78] For a Bi–4.4 mass% Mn alloy, the theoretical volume fraction of MnBi is estimated to be about 21.3%, which gives poor magnetic properties of the alloy. By controlling its migration during solidification, using high-gradient magnetic fields of $\pm 282\ \mathrm{T^2/m}$, the MnBi phase accumulated in one side of the alloy, thereby increasing its volume fraction by above 40%. The hysteresis loops at room temperature for longitudinal sections of the alloys show that the saturation magnetization increased from about 1.6 emu/g without a magnetic field to about 7 emu/g with the gradient magnetic fields. This process provides a method for directly fabricating composite magnetic materials with a high volume fraction of magnetic phases from a dilute master alloy.[66]

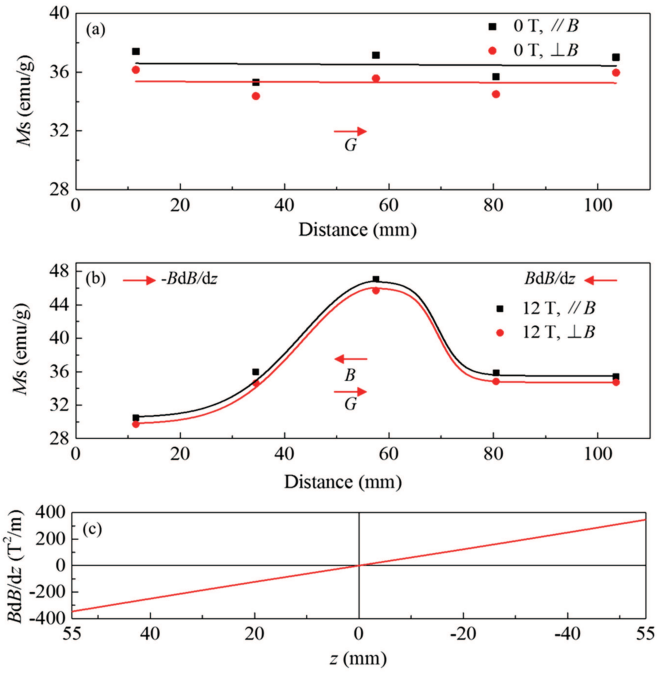


Fig. 16. (color online) Saturation magnetization distribution in Mn–89.7 mass% Sb alloys solidified (a) without and (b) with a magnetic field of 12 T; (c) corresponding $B\mathrm{d}B/\mathrm{d}z$ distribution.[50]

MnSb exhibits a NiAs-type crystal structure and is ferromagnetic below its Curie temperature (587 K).[50,79,80] Associated with its ferromagnetism, MnSb exhibits various physical properties, such as a large magneto-optic effect, a large magnetic anisotropy in the direction of the easy magnetization axis, and a large magnetoresistance.[81] Dong *et al.*[50] applied a symmetrical high-gradient magnetic field to the solidification process of a hypoeutectic Mn–Sb alloy to promote primary MnSb dendrites to distribute along the middle of the alloy. The primary MnSb dendrite content first increased and then decreased along the vertical axis of the alloy. The saturation magnetization of the magnetic field-treated alloy, obtained from the measured hysteresis loops, showed a symmetrical distribution along the sample center. In contrast, the saturation magnetization of the alloy produced without a magnetic field exhibited an almost linear distribution throughout the sample (Fig. 16). This process provides a method for directly fabricating composite magnetic materials with a symmetrical gradient of their magnetic properties.

Giant magnetostrictive materials based on $R\mathrm{Fe_2}$ (R = rare earth element) are some of the most important functional magnetic materials and they have been widely applied in sensors, precision machinery, magnetomechanical transducers, and adaptive vibration-control systems.[82–84] A typical representative is the $\mathrm{Tb_{0.27}Dy_{0.73}Fe_{1.95}}$ alloy. Its giant magnetostrictive phase (Tb, Dy)$\mathrm{Fe_2}$ has an easy magnetization axis along its $\langle 111 \rangle$ direction. Extensive efforts have been made to control the orientation behavior and amount of (Tb, Dy)$\mathrm{Fe_2}$ throughout the material to achieve high magnetostrictive performance. With the aid of high-gradient magnetic fields, Gao *et al.*[56] successfully controlled the distribution of the orientation and amount of the (Tb, Dy)$\mathrm{Fe_2}$ phase in this alloy by modifying its migration behavior. Gradient distributions of saturation magnetization and $\langle 111 \rangle$ orientation throughout the alloys were obtained. Benefitting from these microstructural changes, the magnetostrictive property of the alloy showed a continuous distribution along the magnetic field direction. Applying an external gradient magnetic field during solidification creates new opportunities for the fabrication of graded magnetostrictive materials.

6. Conclusion

From the point of view of solidification of alloys, high-gradient magnetic fields mainly produce a magnetic force, Lorentz force, TEMF, magnetic torque, and magnetic dipole–dipole interaction on materials. The application of a high-gradient magnetic field is found to be a powerful means to control solute and particle migration in alloy melts over a wide range of length scales by coupling these effects. Magnetic field-modified migration can have a profound impact on the development of solidification microstructures and related properties. It is possible to use high-gradient magnetic fields to control material processes related to transport phenomena, such as solidification. Experimental results confirm the possibility that a high-gradient magnetic field can be used to modify or design microstructure of materials that can meet the applications required by advancing technologies.

References

[1] Liu F and Yang G C 2006 *Int. Mater. Rev.* **51** 145

[2] Liu F, Sommer F, Bos C and Mittemeijer E J 2007 *Int. Mater. Rev.* **52** 193
[3] Asta M, Beckermann C, Karma A, Kurz W, Napolitano R, Plapp M, Purdy G, Rappaz M and Trivedi R 2009 *Acta Mater.* **57** 941
[4] Asai S 2000 *Sci. Technol. Adv. Mater.* **1** 191
[5] Watanabe T, Tsurekawa S, Zhao X and Zuo L 2006 *Scr. Mater.* **54** 969
[6] Wang Q, Liu T, Wang K, Wang C J, Nakajima K and He J C 2010 *ISIJ. Int.* **50** 1941
[7] Wang Q, Liu T, Wang K, Gao P F, Liu Y and He J C 2014 *ISIJ. Int.* **54** 516
[8] Akamatsu S and Nguyen-Thi H 2016 *Acta Mater.* **108** 325
[9] Liu T, Wang Q, Zhang H W, Lou C S, Nakajima K and He J C 2011 *J. Mater. Sci.* **46** 1628
[10] Liu T, Wang Q, Zhang H F, Wang K, Pang X J and He J C 2009 *J. Alloy. Compd.* **469** 258
[11] Wang J, Fautrelle Y, Ren Z M, Li X, Nguyen-Thi H, Mangelinck-Noel N, Salloum Abou Jaoude G, Zhong Y B, Kaldre I, Bojarevics A and Buligins L 2012 *Appl. Phys. Lett.* **101** 1331
[12] Ikezoe Y, Hirota N, Nakagawa J and Kitazawa K 1998 *Nature* **393** 749
[13] Alboussiere T, Neubr, A C, Garandet J P and Moreau R 1995 *Magnetohydrodynamics* **31** 228
[14] Sugiyama T, Tahashi M, Sassa K and Asai S 2003 *ISIJ. Int.* **43** 855
[15] Martin J E, Venturini E, Odinek J and Anderson R A 2000 *Phys. Rev. E* **61** 2818
[16] Nakamura H, Takayama T, Uetake H, Hirota N and Kitazawa A K 2005 *Phys. Rev. Lett.* **94** 144501
[17] Wang Y, Hirota N, Okada H, Liu T, Wang Q and Sakka Y 2014 *Key Eng. Mater.* **616** 188
[18] Wang Q, Liu T, Gao A, Zhang C, Wang C J and He J C 2007 *Scr. Mater.* **56** 1087
[19] Lou C S, Wang Q, Wang C J, Liu T, Nakajima K and He J C 2009 *J. Alloy. Compd.* **472** 225
[20] Liu T, Wang Q, Gao A, Zhang C, Wang C J and He J C 2007 *Scr. Mater.* **57** 992
[21] Wang Q, Wang C J, Liu T, Wang K and He J C 2007 *J. Mater. Sci.* **42** 10000
[22] Jin F W, Ren Z M, Ren W L, Deng K, Zhong Y B and Yu J B 2008 *Sci. Technol. Adv. Mater.* **9** 024202
[23] Wang Q, Liu T, Zhang C, Gao A, Li D G and He J C 2009 *Sci. Technol. Adv. Mater.* **10** 014606
[24] Boos A, Lamparter P and Steeb S 1977 *Z. Naturforsch. A* **32** 1222
[25] Zu F Q, Zhu Z G, Guo L J, Qin X B, Yang H and Shan W J 2002 *Phys. Rev. Lett.* **89** 125505
[26] Liu T, Wang Q, Hirota N, Liu Y, Chen S H and He J C 2011 *J. Cryst. Growth* **335** 121
[27] Steinberg D J 1974 *Metall. Mater. Trans.* **5** 1341
[28] Dupree R and Seymour E F W 1972 *Liquid Metals* (New York: Marcel Dekke) p. 461
[29] Jie W 2001 *Sci. Technol. Adv. Mater.* **2** 29
[30] Lan C W and Tu C Y 2002 *J. Cryst. Growth* **237** 1881
[31] Nishida M, Kawamura Y and Yamamuro T 2004 *Mater. Sci. Eng. A* **375–377** 1217
[32] Li Z, Samuel A M, Samuel F H, Ravindran C and Valtierra S 2003 *J. Mater. Sci.* **38** 1203
[33] Loboda-Cackovic J 1997 *Vacuum* **48** 913
[34] Stelian C, Delannoy Y, Fautrelle Y and Duffar T 2004 *J. Cryst. Growth* **266** 207
[35] Hermann R, Behr G, Gerbeth G, Priede J, Uhlemann H, Fischer F and Schultz L 2005 *J. Cryst. Growth* **275** e1533
[36] Suresh S 2001 *Science* **292** 2447
[37] Fukui Y and Watanabe Y 1996 *Metall. Mater. Trans. A* **27** 4145
[38] Yasuda H, Ohnaka I, Kawakami O, Ueno K and Kishio K 2003 *ISIJ. Int.* **43** 942
[39] Utech H P and Flemings M C 1966 *J. Appl. Phys.* **37** 2021
[40] Matthiesen D H, Wargo M J, Motakef S, Carlson D J, Nakos J S and Witt A F 1987 *J. Cryst. Growth* **85** 557
[41] Sha Y G, Su C H and Lehoczky S L 1997 *J. Cryst. Growth* **173** 88
[42] Wang C J, Wang Q, Wang Z Y, Li H T, Nakajima K and He J C 2008 *J. Cryst. Growth* **310** 1256
[43] Yasuda H, Ohnaka I, Kawakami O, Ueno K and Kishio K 2003 *ISIJ. Int.* **43** 942
[44] Li L, Zhang Y D, Esling C, Zhao Z H, Zuo Y B, Zhang H T and Cui J Z 2009 *J. Mater. Sci.* **44** 1063
[45] Li X, Fautrelle Y, Zaidat K, Gagnoud A, Ren Z M, Moreau R, Zhang Y D and Esling C 2010 *J. Cryst. Growth* **312** 267
[46] Yasuda H, Ohnaka I, Ninomiya Y, Ishii R, Fujita S and Kishio K 2004 *J. Cryst. Growth* **260** 475
[47] Wang Q, Lou C S, Liu T, Pang X J, Nakajima K and He J C 2009 *ISIJ. Int.* **49** 1094
[48] Liu T, Wang Q, Wang C J, Li H T, Wang Z Y and He J C 2011 *Metall. Mater. Trans.* **42** 1863
[49] Li X, Ren Z M and Fautrelle Y 2008 *Mater.* **29** 1796
[50] Dong M, Liu T, Liao J, Xiao Y B, Yuan Y and Wang Q 2016 *J. Alloy. Compd.* **689** 1020
[51] Liu T, Wang Q, Gao A, Zhang H W, Wang K and He J C 2010 *J. Mater. Res.* **25** 1718
[52] Liu T, Wang Q, Wang C J, Liu Z G, Yuan Y and He J C 2010 *ISIJ. Int.* **50** 1947
[53] De Rango P, Lees M, Lejay P, Sulpice A and Tournier R 1991 *Nature* **349** 770
[54] Liu T, Wang Q, Gao A, Zhang C, Li D G and He J C 2009 *J. Alloy. Compd.* **481** 755
[55] Liu T, Wang Q, Zhang C, Gao A, Li D G and He J C 2009 *J. Mater. Res.* **24** 2321
[56] Gao P F, Liu T, Dong M, Yuan Y, Wang K and Wang Q 2016 *Funct. Mater. Lett.* **9** 1650003
[57] Liu T, Liu Y, Wang Q, Iwai, K, Gao P F and He J C 2013 *J. Phys. D-Appl. Phys.* **46** 125005
[58] Gao P F, Liu T, Dong M, Yuan Y and Wang Q 2016 *J. Magn. Magn. Mater.* **401** 755
[59] Gao P F, Wang Q, Liu T, Liu Y, Niu S X and He J C 2015 *IEEE Trans. Magn.* **51** 1
[60] Matsushima H, Nohira T, Mogi I and Ito Y 2004 *Surf. Coat. Technol.* **179** 245
[61] Liu T, Gao P F, Dong M, Xiao Y B and Wang Q 2016 *AIP Adv.* **6** 056216
[62] Bishop K J M, Wilmer C E, Soh S and Grzybowski B A 2009 *Small* **5** 1600
[63] Zahn K, Méndezalcaraz J M and Maret G 1997 *Phys. Rev. Lett.* **79** 175
[64] Wirtz D and Fermigier M 1994 *Phys. Rev. Lett.* **72** 2294
[65] Tierno P and Goedel W A 2005 *J. Chem. Phys.* **122** 094712
[66] Wang Q, Lou C S, Liu T, Wei N, Wang C J and He J C 2009 *J. Phys. D: Appl. Phys.* **42** 025001
[67] Lou C S, Wang Q, Liu T, Wei N, Wang C J and He J C 2010 *J. Alloy. Compd.* **505** 96
[68] Li X, Fautrelle Y and Ren Z M 2008 *Acta Mater.* **56** 3146
[69] Li X, Fautrelle Y, Ren Z M, Gagnoud A, Zhang Y D and Esling C 2011 *J. Cryst. Growth* **318** 23
[70] Li X, Li Q Y, Ren Z M, Fautrelle Y, Lu X G, Gagnoud A, Zhang Y D, Esling C, Wang H, Dai Y M and Wang Q L 2013 *J. Alloy. Compd.* **581** 769
[71] Tewari S N, Shah R and Song H 1994 *Metall. Mater. Trans. A: Phys. Metall. Mater. Sci.* **25** 1535
[72] Wang Q, Li D G, Wang K, Wang Z Y and He J C 2007 *Scr. Mater.* **56** 485
[73] Li X, Fautrelle Y and Ren Z M 2007 *Acta Mater.* **55** 3803
[74] Wu M X, Liu T, Dong M, Sun J M, Dong S L and Wang Q 2017 *J. Appl. Phys.* **121** 064901
[75] Chen T and Stutius W 1974 *IEEE Trans. Magn.* **10** 581
[76] Kishimoto M and Wakai K 1975 *Jpn. J. Appl. Phys.* **14** 893
[77] Guo X, Altounian Z and Ström-Olsen J O 1991 *J. Appl. Phys.* **69** 6067
[78] Saha S, Obermyer R T, Zande B J, Chandhok V K, Simizu S, Sankar S G and Horton J A 2002 *J. Appl. Phys.* **91** 8525
[79] Okuda H, Senba S, Sato H, Shimada K, Namatame H and Taniguchi M 1999 *J. Electron. Spectrosc. Relat. Phenom.* **101** 657
[80] Seshu Bai V and Rama Rao K V S 1984 *J. Appl. Phys.* **55** 2167
[81] Akinaga H, Suzuki Y, Tanaka K, Ando K and Katayama T 1995 *Appl. Phys. Lett.* **67** 141
[82] Clark A E and Belson H S 1972 *Phys. Rev. B* **5** 3642
[83] Jiles D C 1994 *J. Phys. D: Appl. Phys.* **27** 1
[84] Wang Q, Liu Y, Liu T, Gao P F, Wang K and He J C 2012 *Appl. Phys. Lett.* **101** 132406